Routledge
Taylor & Francis Group

Journal of Sports Sciences

ISSN: (Print) (Online) Journal homepage: www.tandfonline.com/journals/rjsp20

Evaluation of a time-varying cut-off frequency low-pass filter for assessing knee joint moments and ACL injury risk

Simon Augustus, Blake Rivers, James Brouner & Neal Smith

To cite this article: Simon Augustus, Blake Rivers, James Brouner & Neal Smith (2024) Evaluation of a time-varying cut-off frequency low-pass filter for assessing knee joint moments and ACL injury risk, Journal of Sports Sciences, 42:21, 2039-2051, DOI: 10.1080/02640414.2024.2422724

To link to this article: https://doi.org/10.1080/02640414.2024.2422724

JOURNAL OF SPORTS SCIENCES
2024, VOL. 42, NO. 21, 2039–2051
https://doi.org/10.1080/02640414.2024.2422724

Routledge
Taylor & Francis Group

SPORTS MEDICINE AND BIOMECHANICS

Evaluation of a time-varying cut-off frequency low-pass filter for assessing knee joint moments and ACL injury risk

Simon Augustus[a], Blake Rivers[a], James Brouner[a] and Neal Smith[b]

[a]Department of Applied and Human Science, Faculty of Health, Sciences, Social Care and Education, Kingston University, London, UK; [b]School of Sport and Exercise Sciences, University of Chichester, Chichester, UK

ABSTRACT

Conventional low-pass filtering of 3D motion capture signals prior to estimating knee joint moments and ACL injury risk has known limitations. This study aimed to evaluate the fractional Fourier filter (FrFF), which employs a time-varying cut-off frequency, for assessing peak knee moments during common ACL injury risk screening tasks. Ground reaction force and motion data were collected from 23 team sport athletes performing 45° unanticipated sidesteps and drop jumps. Peak knee abduction, internal rotation and non-sagittal moments were estimated using inverse dynamics after five different low-pass filter approaches were applied (FrFF vs. four variations of a fourth-order Butterworth filter). The FrFF produced peak knee moments larger than "matched" (i.e. force and motion cut-off frequencies were equivalent) and closer to "unmatched" (i.e. force and motion cut-offs were different) Butterworth filter approaches and removed problems with representing foot-to-ground impact peaks. Participants with larger peak moments were identified as "at risk" of injury irrespective of filter approach, but the FrFF identified "at risk" classifications conventional approaches did not. Preliminary evidence suggests that the FrFF displays enhanced sensitivity to movement strategies that induce high knee loads. This was most evident for sidestepping, with more research warranted to optimise the FrFF for drop jumps.

ARTICLE HISTORY
Received 12 February 2024
Accepted 22 October 2024

KEYWORDS
Inverse dynamics; anterior cruciate ligament; fractional Fourier filter; screening; classification

Introduction

Anterior cruciate ligament (ACL) ruptures are devastating knee injuries that incur huge financial (Abram et al., 2018) and personal cost (Filbay et al., 2022). Surgical reconstruction remains the gold standard treatment, but only 33–78% of reconstructed athletes return to pre-injury activity levels (Weir et al., 2019). Those who do not return to participation are 4–6 times more likely to develop osteoarthritis (Poulsen et al., 2019) and may suffer negative psychological consequences related to physical inactivity (Filbay et al., 2022). Given injury rates continue to grow (Saxby et al., 2023) and ~70% of injuries occur in non-contact situations (Krosshaug et al., 2007), classification of "at risk" individuals offers opportunities for targeted interventions to reduce injury rates. Numerous risk factors have been identified (e.g., hormonal, genetic and anatomical; Myer et al., 2008), but risk reduction research has focused on biomechanical factors, as these are more easily modified through physical intervention (Weir et al., 2019).

Estimates of knee loads during high impact, multiplanar activities such as drop jumps and sidestep cutting have been used as indicators of ACL injury risk (Hewett et al., 2005; Kristianslund & Krosshaug, 2013). Specifically, since ACL injuries likely occur ~50–60 ms following initial foot-to-ground contact (Cerulli et al., 2003), peak moments observed during the initial weight acceptance phase of these tasks have been used to infer injury risk (Weir, 2021). However, whilst large anterior tibial shear forces coupled with frontal and transverse moments have been associated with ACL strain in cadaveric and simulation studies (Markolf et al., 1995; Ueno et al., 2020), using resultant joint moments derived from 3D motion capture as surrogates of ACL strain (and thus injury risk) have been contentious. Elevated peak knee abduction moments (PKAM) (Hewett et al., 2005) and internal rotation moments (PIRM) (Chinnasee et al., 2018) have shown to be predictive of ACL injury risk, and peak non-sagittal moments (PNSM; vector magnitude of knee abduction and internal rotation moments) have identified "at risk" individuals where PKAM and PIRM alone could not (Robinson et al., 2021). In contrast, a few prospective studies (Krosshaug et al., 2016; Leppänen et al., 2017) and a meta-analysis (Cronström et al., 2020) have contended these variables have no predictive utility for ACL injury.

One reason for equivocal findings is variation in processing required to derive joint loads. Knee moments estimated from 3D motion capture and inverse dynamics rely on obtaining valid ground reaction forces (GRFs), segment inertial parameters and lower limb kinematics (e.g., velocities and accelerations). While the former are relatively simple to determine, accurate acquisition of kinematic parameters is challenging. Noise associated with soft-tissue artefact and 3D system precision limitations (e.g., electronic noise, marker tracking errors) is amplified when body segment positions and orientations are differentiated. Marker and GRF signals are thus often low-pass filtered (e.g., Butterworth digital filter) before calculating joint moments (Derrick et al., 2020). However, transition from aerial

CONTACT Simon Augustus s.augustus@kingston.ac.uk Department of Applied and Human Sciences, Kingston University, Penrhyn Road, London KT1 2EE, UK
Supplemental data for this article can be accessed online https://doi.org/10.1080/02640414.2024.2422724

to foot-to-ground contact phases of drop jump and sidestepping induces rapid expansion of kinematic frequency content and large lower-limb segment acceleration impact peaks. If these signals are not appropriately treated, they can confound knee loads and injury risk classifications.

Some studies have justified filtering marker signals at lower cut-off frequencies (e.g., 5–20 hz) than GRFs (e.g., 50–150 hz) (Hewett et al., 2005; Sigward & Powers, 2007; Ueno et al., 2020), but there are concerns so-called "unmatched" approaches create spurious peaks in computed joint moments (Kristianslund et al., 2012). Such an approach retains physiologically meaningful impact peaks in GRFs but removes them from kinematic signals, leading to inconsistencies in the equations of motion that manifest as errors in joint kinetics (Bisseling & Hof, 2006). The prevailing convention has thus been to filter marker and GRF signals at the same lower "matched" cut-off frequency (e.g., 10 and 10, or 20 and 20 hz; Krosshaug et al., 2016; Robinson et al., 2021; Weir et al., 2019). This ensures no discrepancy in the frequency content of input signals and may result in more accurate representations of knee moments (Bisseling & Hof, 2006; van den Bogert & de Koning, 1996). Unfortunately, this approach has also been criticised as it removes important impact peaks from both kinematic and kinetic signals following foot-to-ground contact (Roewer et al., 2014). As previously noted, since non-contact ACL injuries occur soon ~50–60 ms initial ground contact (i.e., during weight acceptance; Cerulli et al., 2003), this is problematic as over-smoothed input variables can also distort peak knee moment estimates.

If conventional low-pass filters cannot adequately represent knee loads during ACL injury risk screening tasks, their application should be reviewed. One alternative is to use a filter with a time-varying cut-off frequency. Increasing cut-off frequencies when foot-to-ground contact induces sudden (de)acceleration of the lower limbs can ensure optimal retention of physically meaningful impact peaks and removal of noise from kinematic and GRF signals across the entire task. Such techniques are widely used in optics, speech and music processing, and mechanical vibrations analysis (Ozaktas et al., 1999; Wei & Ran, 2013), but have been largely ignored in human movement studies. Methods based on wavelet transforms (Wachowiak et al., 2000), singular spectrum analysis (Alonso et al., 2005) and the Wigner distribution (Georgakis et al., 2002) have been used in biomechanics, but problems regarding computational complexity (e.g., non-linear algorithms) and ease of implementation has meant they are not widely adopted.

To address the former, Georgakis and Subramaniam (2009) proposed the fractional Fourier filter (FrFF). The FrFF leverages the fractional Fourier transform to render a faster, more linear algorithm; and employs a triangular, time-varying cut-off frequency boundary that permits retention of higher frequency kinematic (and/or kinetic) content during impact (e.g., foot-to-ground contact; Figure 1). Filter parameters are chosen to represent the impact characteristics (i.e., magnitude and duration) of a given signal and create an optimal filter solution (Georgakis & Subramaniam, 2009). The FrFF has outperformed conventional low-pass (e.g., Butterworth filters) and other time-frequency filter methods for a) estimating lower leg accelerations during drop landings (Georgakis & Subramaniam, 2009) and b) representing changes in kick leg kinematics during foot-to-ball contact of ball kicking (Augustus et al., 2020). To date, however, the efficacy of the FrFF for determining knee joint kinetics and classifying ACL injury risk remains to be verified. If more precise estimates of lower leg kinematics (e.g., foot and shank accelerations) and GRFs can be derived, it is logical that joint moment estimates and injury risk classifications would also be more precise. Correctly identifying "at risk" individuals is paramount if attempts to mitigate ACL injury rates are to be successful. The first aim of this study was thus to compare the FrFF with conventional "matched" and "unmatched" Butterworth low-pass filter approaches for deriving peak knee joint moments during ACL injury risk screening tasks. A secondary aim was to assess how filter approach affects injury risk classifications.

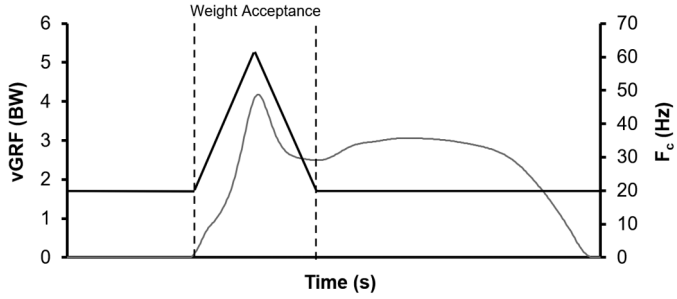

Figure 1. Illustration of the FrFF triangular cut-off frequency filter boundary. The time-varying cut-off frequency (black line; F_c) was designed to increase during weight acceptance. That is, between initial ground contact (vGRF > 25 N; first dashed vertical line) and the first trough in vGRF following the impact peak (minimum vGRF value between impact and active peaks; second dashed vertical line). These events denote the width of the FrFF triangular filter boundary and correspond to the duration of weight acceptance, as shown.

Materials and methods

Participants and study design

Twenty-three recreationally active men and women (13 men, 27.5 ± 4.3 years, 83.9 ± 6.5 kg, 1.80 ± 0.05 m; 10 women, 23.9 ± 3.2 years, 65.9 ± 11.0 kg, 1.68 ± .07 m) were recruited from team sports (e.g., soccer, netball, field hockey). All were free from injury 12 months preceding data collection and participated in their sport at least twice per week. Those with previous confirmed ACL injury were excluded and approval granted by the University's ethics committee (MR-3030). A cross-sectional approach was adopted whereby peak knee joint moments associated with ACL injury risk were estimated during common screening tasks after application of five different low-pass filters. For this repeated measures design, *a priori* analysis indicated a sample of 21 participants would achieve statistical power of 0.95 with $\alpha = 0.05$, expected strong correlation between repeated measures ($r = 0.7$) and medium effect sizes ($\eta_p^2 = 0.06$; Kristianslund et al., 2012; G*Power 3.1.9.7).

Data collection and modelling

After 10 min of warm-up and familiarisation, participants completed single leg drop jump (SLDJ), bilateral drop jump (BDJ) and unanticipated sidestep change of directions (SS) in

a random order. The SLDJ and BDJ were performed by stepping off a 30 cm box (Hewett et al., 2005) and exploding vertically into a maximal vertical jump upon contact with a force platform (1000 hz; 9286C, Kistler, Switzerland). An overhead target ensured maximal effort. Three repetitions were performed on each leg for SLDJ, and the dominant leg (i.e., the leg predominantly used to kick a ball) contacted the force platform for the BDJ. For SS, participants performed a 45° sidestep with the cutting step on the force platform. A straight 7 m approach was used and timing gates (Smartspeed Plus, VALD Ltd., UK) determined approach velocities 2.9 m before the force platform. Breaking the gates triggered a visual LED stimulus that indicated the required change of direction at random. This afforded approximately 400 ms to react to the stimulus and perform the task. Only trials with approach velocities of 4–5 m/s (Vanrenterghem et al., 2012) and where the entire stance foot contacted the force platform were included. Three successful trials were performed in each direction (left and right).

Fifty-two spherical reflective markers (12.6 mm diameter) determined lower-limb and torso kinematics using a 10-camera three-dimensional motion capture system (250 hz; Vicon T40S, OMG Plc, UK). This sampling frequency replicated those used in previous studies. Static calibration defined neutral pose of feet, shanks, thighs, pelvis and a torso in Visual 3D (v2023.03.01; C-Motion, USA). All segments were rigid geometric volumes scaled to participant height and mass, with inertial parameters according to de Leva (1996). The feet were modelled as single rigid bodies using malleoli markers to define the proximal diameter and ankle joint centre, and the second and fifth metatarsal markers to define the distal radius. The shanks used femoral epicondyle markers to define the proximal diameter and knee joint centre, and malleoli markers to define the distal diameter. Proximal and distal thighs were defined using the method of Bell et al. (1990) to estimate the hip joint centre, and femoral epicondyles, respectively. Anatomical coordinate systems were thus created at the proximal end of each segment (i.e., joint centre locations), where positive Z pointed superiorly with the long axis of the segment, positive X pointed towards the lateral calibration marker, and positive Y anteriorly as the cross product of ZX. Segment motion was tracked in six degrees of freedom using triad marker clusters attached to thighs and shanks (Cappozzo et al., 1995); and individual markers placed on the head of second and fifth metatarsals, and posterior calcaneus for the feet.

Low-pass filter approaches

Marker trajectories and GRFs were exported to Visual 3D (v2023.03.01; C-Motion, USA) and processed for each low-pass filter approach. To represent methods conventionally used to filter signals before estimating knee joint loads, four combinations of a fourth-order, zero lag, Butterworth low-pass filter were used. Two were "matched" (10–10 hz and 20–20 hz) and two "unmatched" (10–50 hz and 20–50 hz), where the first and second values in each combination refer to kinematic (marker) and kinetic (GRF and centre of pressure) cut-off frequencies, respectively. These combinations were chosen to closely represent those most commonly adopted in previous study of ACL injury risk (e.g., Kristianslund et al., 2012; Hewett et al., 2005; Ueno et al., 2020; Vanrenterghem et al., 2012).

The fifth approach filtered ground-contacting foot and shank markers using the FrFF (Georgakis & Subramaniam, 2009). A triangular cut-off frequency boundary was designed to optimise retention of physiologically meaningful impact related frequency content during weight acceptance (Figure 1). Each marker was processed separately so the peak cut-off frequency corresponded temporally to the instance of its own peak acceleration (i.e, apex of the triangle). Specifically, for all tasks, a pre-ground contact cut-off frequency of 20 hz linearly increased at the instance of initial ground contact (i.e, vertical GRF > 25 N) to a peak of 60 hz at the time of the peak marker acceleration, and linearly decreased back to 20 hz at the instance of the first trough in the vertical GRF following the impact peak (i.e., lowest vertical GRF value between impact and active peaks). These events were defined automatically using a Visual 3D pipeline so the temporal width of the base of the triangle corresponded to the duration of weight acceptance from unprocessed signals on a trial by trial basis.

The pre- and post-weight acceptance cut-off frequency (20 hz) and the peak frequency at the apex of the triangle (60 hz) were determined by pilot work conducted on a subsample of the main analysis, and these parameters did not vary across trials and tasks. To select these parameters, residual (Winter, 2009) and frequency analyses (frequency at which 95% of content was retained) were performed on marker trajectories truncated to each phase of each task (i.e., on each pre-weight acceptance, weight acceptance and post-weight acceptance separately; Augustus & Smith, 2023). For peak cut-off frequencies during weight acceptance, optimally determined values of 20–60 hz were evident across marker locations (i.e., foot vs. shank) and screening tasks (i.e., BDJ vs. SS) (Augustus & Smith, 2023). Given this variation, we chose the highest value to limit loss of physiologically meaningful signal. However, we acknowledge this meant some noise might have been retained in some instances. Optimally determined pre- and post-weight acceptance cut-off values also varied between 3 and 20 hz (Augustus & Smith, 2023). Again, the highest value was chosen to ensure limited loss of physically meaningful signal. This was not deemed problematic as joint moment estimates were not of interest during these phases of the tasks. The GRFs and centre of pressure data were filtered using these same parameters to help ensure no discrepancy in the frequency content of the kinematic and kinetic signals (Bisseling & Hof, 2006).

All conventional Butterworth filtering was performed in Visual 3D, and for the FrFF by exporting unprocessed marker trajectories and kinetic data to Matlab (R2022a, MathWorks, USA), where custom written scripts processed the data. Examples of the scripts can be found at GitHub: s-augustus04/Fractional-Fourier-Low-Pass-Filter. FrFF processed marker trajectories and GRFs were re-imported back to Visual 3D where peak knee moment variables were derived.

Data and statistical analyses

For all trials, resultant knee joint moments were derived using standard Newton–Euler inverse dynamics in Visual 3D. These moments were resolved to the proximal (thigh)

segment and normalised to body mass. PKAM and PIRM were determined during weight acceptance from frontal and transverse time-series moments, respectively, and reported as external moments. In absence of knee abduction or internal rotation moments, the smallest adduction or external rotation moment was used. PNSM was determined from the vector magnitude of frontal and transverse moments (Robinson et al., 2021). All peak moments were averaged across each participant's three trials per task to obtain a mean response, and these were used for further analysis.

Peak moment data were assessed for normality using the Shapiro–Wilks test. Then, one-way repeated-measures ANOVAs evaluated differences across filter approach. If sphericity was violated, Greenhouse-Geisser adjustments were used. Alpha was Bonferroni adjusted for multiple comparisons (5 tasks × 3 peak moment variables; $\alpha = 0.003$). For significant main effects, post hoc Bonferroni paired t-tests assessed differences between each conventional filter approach and the FrFF ($N = 4$ paired comparisons per variable, $\alpha = 0.013$). This method was chosen as a balanced approach to mitigate against Type I (i.e., family-wise error inflation) and Type II error (i.e., reduced statistical power) (Toothaker, 1993). Spearman's rank correlations assessed consistency in participant rankings for each peak moment variable (0–0.2 = no correlation, 0.2–0.4 = weak, 0.4–0.7 = moderate, 0.7–1.0 = strong). All statistical comparisons were performed in JASP (0.16.3, https://jasp-stats.org/). To evaluate if filter approach influenced injury risk classification, a risk threshold of sample mean + 1.6 standard deviations (SD) was used (Robinson et al., 2014). If any participant's mean response for a peak moment exceeded this threshold, they were classified as "at risk" of ACL injury. This approach was based on recommendations for similar populations (Chinnasee et al., 2018) and because risk classifications have been shown as robust between mean + 1 SD to + 2 SD (Robinson et al., 2021).

Results

Main effects were identified across all screening tasks ($p < 0.003$, Table 1). The exception was PIRM in the left leg SLDJ. Generally, the FrFF produced larger peak moments than matched 10–10 hz and 20–20 hz approaches, with medium to large effect sizes ($d > 0.60$, $p < 0.013$; Table 2). These differences were more pronounced in SS compared to BDJ and SLDJ (Table 2, Figure 2). Peak moments from unmatched approaches were mostly not different to the FrFF with small to medium effect sizes (d = 0.10–0.60). However, 10–50 hz PKAM and PNSM in the right leg SLDJ, and 20–50 hz PKAM and PNSM in the left leg SLDJ were smaller than the FrFF ($p < 0.013$), with small to large effects (Table 2, Figure 2). Like the matched approaches, the magnitude of differences between FrFF and unmatched approaches was more pronounced in the SS compared to drop jumps (Table 2).

Spearman's correlations showed moderate to strong associations between participant rankings for FrFF and conventional filter approaches (Table 3). Irrespective of task, participant rankings were more consistent between the FrFF and unmatched approaches, with weakest correlations between FrFF and 10–10 hz. There were some exceptions, notably where FrFF showed better consistency with 20–20 hz than 10–50 hz for PKAM in both SLDJ tasks. Correlations between FrFF and conventional approaches in SS were stronger for PKAM than for PIRM and PNSM. This consistency extended across all filter approaches, with little variation in participant rankings (Figure 3). In contrast, for drop jumps, correlations between FrFF and conventional approaches were stronger for PIRM, compared to PKAM and PNSM. This consistency is also highlighted across all filter approaches (Figure 3).

For injury risk classifications in SS, matched approaches were most conservative, with more individuals classified as "at risk" by FrFF and 20–50 hz (Figure 2). Unmatched approach classifications were closer to the FrFF, but the FrFF still uniquely identified individuals that were not classified as "at risk" in

Table 1. Mean (SD) peak knee abduction (PKAM), internal rotation (PIRM) and non-sagittal moments (PNSM) (Nm/kg) in each filter approach, across screening tasks. * indicates a repeated measures ANOVA significant main effect ($p < 0.003$). η_p^2 = partial eta squared effect sizes (>0.01 = small, > 0.06 = medium and > 0.13 = large).

	FrFF	10-10	10-50	20-20	20-50	p-value	η_p^2
Sidestep Left Leg							
PKAM	0.88 (0.74)	0.20 (0.36)	0.60 (0.73)	0.45 (0.59)	0.70 (0.64)	<0.001*	0.47
PIRM	0.14 (0.08)	0.06 (0.05)	0.11 (0.07)	0.10 (0.06)	0.14 (0.06)	<0.001*	0.47
PNSM	1.15 (0.58)	0.55 (0.21)	1.02 (0.40)	0.77 (0.45)	0.99 (0.48)	<0.001*	0.54
Sidestep Right Leg							
PKAM	1.33 (0.91)	0.54 (0.54)	1.22 (0.80)	0.86 (0.71)	1.15 (0.86)	<0.001*	0.62
PIRM	0.16 (0.11)	0.03 (0.08)	0.11 (0.09)	0.08 (0.06)	0.14 (0.08)	<0.001*	0.53
PNSM	1.47 (0.80)	0.71 (0.41)	1.32 (0.70)	1.00 (0.60)	1.29 (0.76)	<0.001*	0.61
Bilateral Drop Jump							
PKAM	0.51 (0.35)	0.31 (0.29)	0.48 (0.36)	0.49 (0.32)	0.52 (0.32)	<0.001*	0.45
PIRM	0.12 (0.11)	0.08 (0.09)	0.11 (0.10)	0.11 (0.10)	0.13 (0.10)	<0.001*	0.57
PNSM	0.61 (0.42)	0.40 (0.34)	0.57 (0.37)	0.58 (0.44)	0.62 (0.42)	<0.001*	0.39
Single Leg Drop Jump Left Leg							
PKAM	0.37 (0.26)	0.03 (0.15)	0.24 (0.23)	0.17 (0.17)	0.22 (0.19)	<0.001*	0.51
PIRM	0.14 (0.11)	0.10 (0.10)	0.13 (0.11)	0.12 (0.10)	0.13 (0.11)	<0.027	0.12
PNSM	0.71 (0.23)	0.49 (0.22)	0.64 (0.25)	0.62 (0.24)	0.62 (0.24)	<0.001*	0.47
Single Leg Drop Jump Right Leg							
PKAM	0.46 (0.30)	0.08 (0.16)	0.22 (0.17)	0.27 (0.29)	0.31 (0.28)	<0.001*	0.51
PIRM	0.19 (0.18)	0.14 (0.17)	0.16 (0.17)	0.18 (0.18)	0.23 (0.19)	<0.001*	0.43
PNSM	0.97 (0.52)	0.67 (0.42)	0.83 (0.42)	0.85 (0.46)	0.89 (0.47)	<0.001*	0.41

Table 2. Pairwise mean differences (95% CI) and post-hoc Bonferroni t-tests for the FrFF with each conventional filter approach, across screening tasks. Peak knee abduction (PKAM), internal rotation (PIRM) and non-sagittal moments (PNSM). * indicates significantly different to FrFF ($p < 0.013$). Cohen's d: trivial $d < 0.2$, small $d = 0.2–0.5$, medium $d = 0.5–0.8$ and large $d > 0.8$.

	FrFF vs 10–10		FrFF vs 10–50		FrFF vs 20–20		FrFF vs 20–50	
	Mean Diff (95% CI)	p-value (d)	Mean Diff (95% CI)	p-value (d)	Mean Diff (95% CI)	p-value (d)	Mean Diff (95% CI)	p-value (d)
Sidestep Left Leg								
PKAM	0.68 (0.39, 0.97)	<0.001* (1.08)	0.27 (0.04, 0.60)	0.119 (0.44)	0.43 (0.21, 0.64)	<0.001* (0.68)	0.18 (0.02, 0.38)	0.112 (0.29)
PIRM	0.08 (0.04, 0.12)	<0.001* (1.25)	0.03 (0.01, 0.08)	0.226 (0.52)	0.04 (0.01, 0.07)	0.005* (1.14)	0.01 (−0.02, 0.04)	1.000 (0.13)
PNSM	0.61 (0.31, 0.90)	<0.001* (1.34)	0.13 (0.12, 0.37)	1.000 (0.29)	0.38 (0.16, 0.60)	<0.001* (0.87)	0.16 (−0.03, 0.36)	0.140 (0.38)
Sidestep Right Leg								
PKAM	0.79 (0.46, 1.12)	<0.001* (1.02)	0.12 (−0.12, 0.33)	1.000 (0.14)	0.46 (0.20, 0.72)	<0.001* (0.60)	0.18 (0.01, 0.35)	0.041 (0.27)
PIRM	0.12 (0.07, 0.18)	<0.001* (1.47)	0.06 (0.01, 0.09)	0.017 (0.54)	0.08 (0.02, 0.13)	0.002* (0.88)	0.02 (−0.03, 0.06)	1.000 (0.19)
PNSM	0.76 (0.45, 1.01)	<0.001* (1.14)	0.15 (−0.04, 0.33)	0.235 (0.22)	0.47 (0.20, 0.73)	<0.001* (0.70)	0.18 (0.02, 0.34)	0.025 (0.26)
Bilateral Drop Jump								
PKAM	0.20 (0.11, 0.30)	<0.001* (0.62)	0.03 (−0.07, 0.13)	1.000 (0.09)	0.03 (−0.07, 0.12)	1.000 (0.08)	−0.01 (−0.09, 0.07)	1.000 (0.08)
PIRM	0.04 (0.02, 0.05)	<0.001* (0.39)	0.01 (0.00, 0.02)	0.138 (0.10)	0.01 (−0.01, 0.02)	1.000 (0.03)	0.00 (−0.02, 0.01)	1.000 (−0.03)
PNSM	0.21 (0.12, 0.31)	<0.001* (0.54)	0.04 (−0.08, 0.17)	1.000 (0.11)	0.03 (−0.07, 0.14)	1.000 (0.08)	−0.01 (−0.10, 0.08)	1.000 (−0.03)
Single Leg Drop Jump Left Leg								
PKAM	0.34 (0.21, 0.47)	<0.001* (1.57)	0.13 (0.00, 0.25)	0.049 (0.57)	0.20 (0.09, 0.31)	<0.001* (0.92)	0.18 (0.06, 0.29)	<0.001* (0.81)
PIRM	0.05 (0.03, 0.07)	N/A (0.42)	0.02 (0.00, 0.03)	N/A (0.16)	0.02 (−0.01, 0.04)	N/A (0.19)	0.03 (−0.04, 0.10)	1.000 (0.28)
PNSM	0.22 (0.13, 0.31)	<0.001* (0.94)	0.08 (−0.02, 0.17)	0.171 (0.32)	0.10 (0.01, 0.19)	0.009* (0.42)	0.10 (0.03, 0.16)	0.012* (0.40)
Single Leg Drop Jump Right Leg								
PKAM	0.39 (0.27, 0.54)	<0.001* (1.54)	0.24 (0.08, 0.40)	<0.001* (0.96)	0.19 (0.05, 0.32)	0.002* (0.79)	0.15 (0.03, 0.28)	0.014 (0.61)
PIRM	0.05 (0.02, 0.08)	<0.001* (0.28)	0.03 (0.00, 0.05)	0.023 (0.15)	0.02 (−0.01, 0.04)	0.319 (0.10)	0.01 (−0.01, 0.03)	1.000 (0.10)
PNSM	0.30 (0.17, 0.43)	<0.001* (0.65)	0.14 (0.02, 0.26)	0.012* (0.30)	0.12 (−0.01, 0.25)	0.111 (0.25)	0.08 (−0.03, 0.19)	0.386 (0.17)

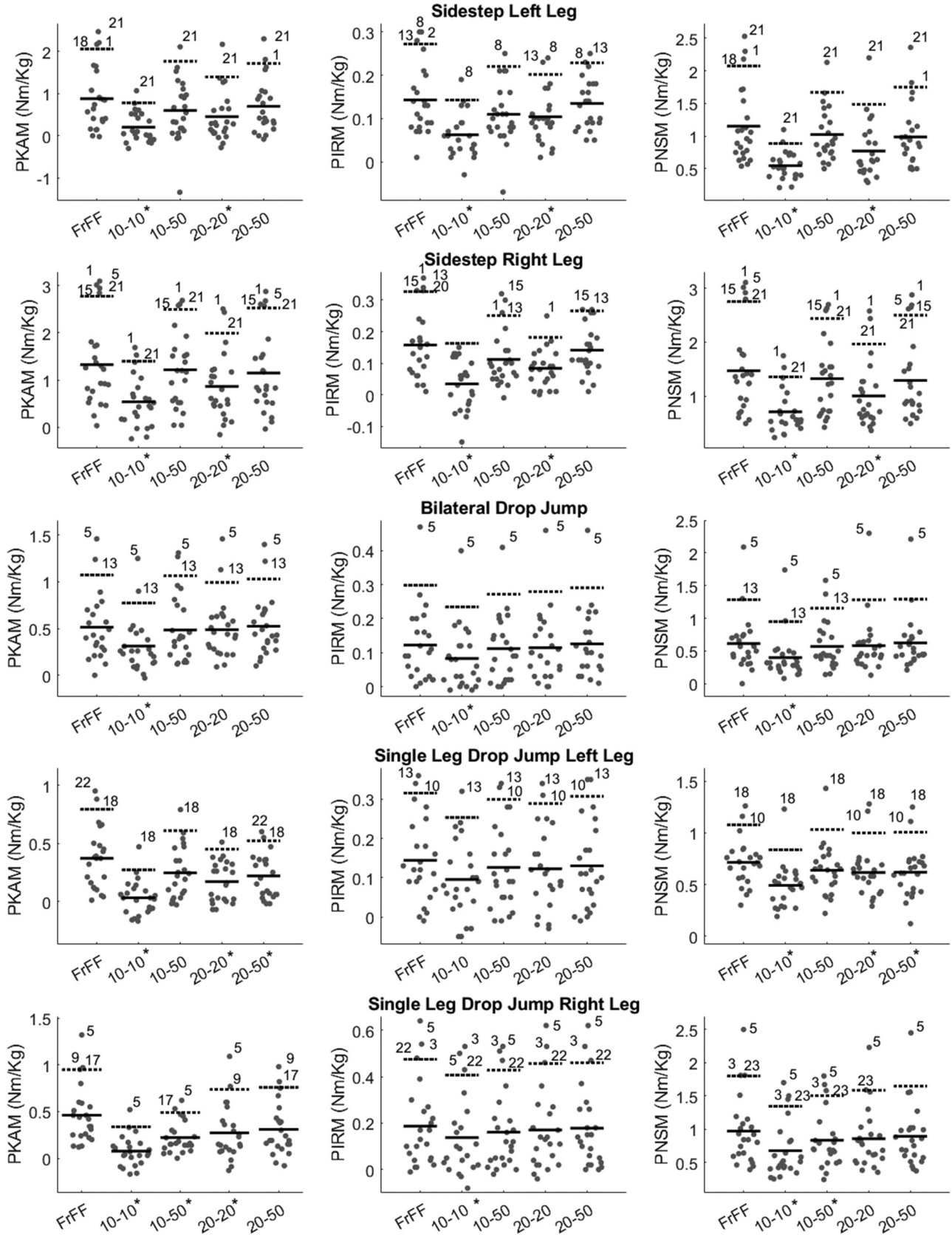

Figure 2. Swarm plots showing peak knee abduction (PKAM, first column), internal rotation (PIRM, second column) and non-sagittal moments (PNSM, third column) for each filter approach across the screening tasks. Horizontal solid lines indicate mean values per filter approach and dashed lines the corresponding injury risk threshold (mean + SD*1.6). Participant numbers printed above each threshold highlight individuals classed as "at risk" for that filter approach. The * next to x-axis labels indicates that filter approach was significantly different to the FrFF ($p < 0.013$).

Table 3. Spearman's rank correlations (95% CI) between the FrFF and conventional filter approaches for peak knee abduction (PKAM), internal rotation (PIRM) and non-sagittal moments (NSM), across screening tasks.

	FrFF vs 10–10	FrFF vs 10–50	FrFF vs 20–20	FrFF vs 20–50
Sidestep Left Leg				
PKAM	0.859 (0.675, 0.939)	0.889 (0.731, 0.964)	0.944 (0.857, 0.973)	0.934 (0.788, 0.985)
PIRM	0.561 (0.115, 0.850)	0.742 (0.395, 0.899)	0.770 (0.481, 0.919)	0.881 (0.680, 0.963)
PNSM	0.632 (0.250, 0.845)	0.768 (0.462, 0.915)	0.699 (0.379, 0.867)	0.808 (0.530, 0.925)
Sidestep Right Leg				
PKAM	0.777 (0.472, 0.919)	0.884 (0.706, 0.957)	0.825 (0.564, 0.934)	0.919 (0.773, 0.986)
PIRM	0.680 (0.413, 0.854)	0.829 (0.618, 0.950)	0.724 (0.419, 0.901)	0.851 (0.590, 0.965)
PNSM	0.772 (0.381, 0.906)	0.893 (0.708, 0.961)	0.731 (0.361, 0.919)	0.886 (0.660, 0.975)
Bilateral Drop Jump				
PKAM	0.874 (0.706, 0.950)	0.882 (0.694, 0.951)	0.841 (0.612, 0.946)	0.864 (0.635, 0.966)
PIRM	0.947 (0.818, 0.988)	0.950 (0.820, 0.989)	0.937 (0.795, 0.985)	0.958 (0.846, 0.991)
PNSM	0.816 (0.573, 0.937)	0.797 (0.531, 0.937)	0.778 (0.505, 0.926)	0.815 (0.534, 0.957)
Single Leg Drop Jump Left Leg				
PKAM	0.671 (0.390, 0.864)	0.727 (0.470, 0.892)	0.754 (0.432, 0.927)	0.869 (0.693, 0.930)
PIRM	0.902 (0.727, 0.973)	0.966 (0.997, 0.992)	0.943 (0.797, 0.981)	0.957 (0.852, 0.995)
PNSM	0.667 (0.256, 0.899)	0.695 (0.273, 0.916)	0.665 (0.282, 0.871)	0.828 (0.500, 0.969)
Single Leg Drop Jump Right Leg				
PKAM	0.457 (0.063, 0.731)	0.432 (0.011, 0.750)	0.582 (0.172, 0.835)	0.614 (0.220, 0.858)
PIRM	0.969 (0.887, 0.994)	0.976 (0.919, 0.994)	0.950 (0.826, 0.990)	0.956 (0.840, 0.993)
PNSM	0.826 (0.532, 0.965)	0.912 (0.721, 0.983)	0.814 (0.451, 0.974)	0.839 (0.480, 0.990)

any other approach (left leg SS = participant 18 for PKAM and PNSM, and participant 2 for PIRM; right leg SS = participant 20 for PIRM). No conventional approach identified an "at risk" case where the FrFF did not make the same classification. For drop jumps, classifications were more consistent (Figure 2). All approaches identified the same individuals for PKAM and PIRM in the BDJ (participants 5 and 13), but 20–20 hz and 20–50 hz precluded participant 13 as "at risk" for PNSM. Similar to SS, lower cut-off frequency combinations precluded some individuals compared to the FrFF in the SLDJ. This was mostly for 10–10 hz, but also 10–50 hz did not classify individuals captured by a) the FrFF and 20–50 hz for the left leg SLDJ PKAM (participant 22) and b) FrFF, 20–50 hz and 20-20 hz for left leg PNSM (participant 10). The FrFF did not uniquely identify any "at risk" individual compared to conventional approaches for the SLDJ, but like for the SS, conventional approaches did not identify any individual as "at risk" where the FrFF did not make the same classification.

Discussion

The first aim of this study was to compare the FrFF with conventional Butterworth "matched" and "unmatched" low-pass filter approaches for deriving peak knee joint moments during ACL injury risk screening tasks. Generally, the FrFF produced PKAM, PIRM and PNSM values larger than those from "matched" approaches and closer to those from "unmatched" approaches. This was expected, as lower and matched cut-off frequencies are known to produce smaller and smoother knee moment profiles (Kristianslund et al., 2012; Roewer et al., 2014). Such methods ensure the frequency content of kinematic and GRF signals are consistent, but at the cost of removing physiologic impact peaks that may be important for understanding ACL injury risk (Roewer et al., 2014). In contrast, unmatched approaches retained impact peaks in the GRFs, resulting in larger peak knee moments consistent with those previously reported (Kristianslund et al., 2012). However, since impact peaks were removed from corresponding kinematic signals, the resulting moments may suffer from error owing to discrepancies in the frequency content of the signals. Bisseling and Hof (2006) highlighted how such errors manifest, but Roewer et al. (2014) contend that some individuals may not be affected by this problem. To date, no study has provided an in-depth analysis to determine the extent of this issue. In comparison, the FrFF used a time-varying cut-off frequency to ensure a) important lower limb frequency content was retained in both kinematic and GRF signals following foot-to-ground contact and b) no discrepancies in the frequency content of these signals. Larger peak moments observed for the FrFF were thus solely determined by experimental data and were not contaminated by error associated with inconsistencies in the frequency content of kinematic and kinetic inputs to the equations of motion. Previous work has shown the benefits of using time-varying cut-off frequencies over conventional low-pass filters to estimate lower leg kinematics during foot-to-ground contact of drop landing and running tasks (Davis & Challis,

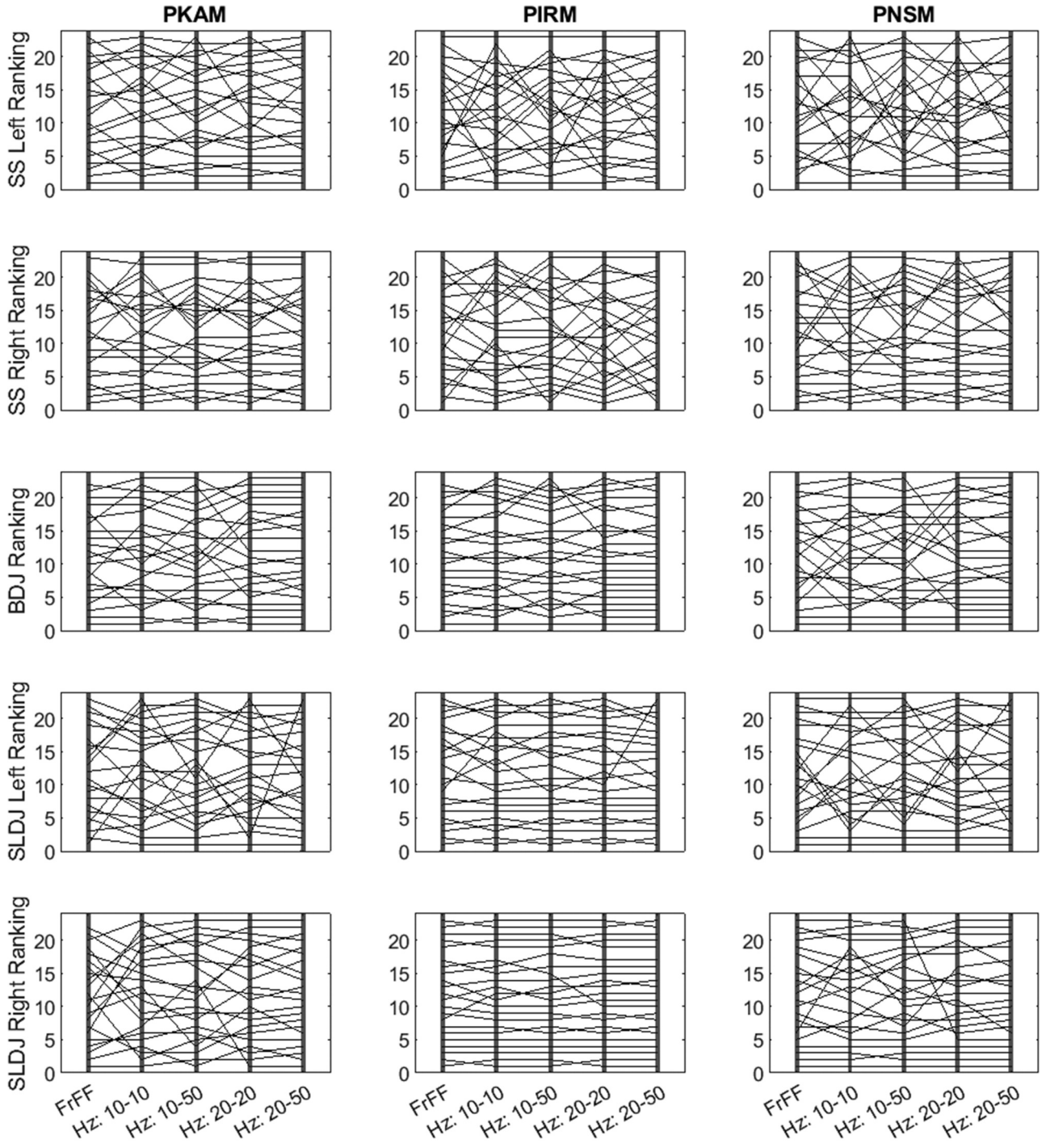

Figure 3. Participant rankings (1–23) for peak knee abduction (PKAM), internal rotation (PIRM) and non-sagittal moments (PNSM) within filter approach and screening task. Each line connects an individual's ranking across filter approach. Horizontal lines show consistent rankings across within filter approach and line crossings inconsistent rankings within filter approach. SS = sidestep change of direction, BDJ = bilateral drop jump, SLDJ = single leg drop jump.

2021; Georgakis & Subramaniam, 2009; Georgakis et al., 2002). From a theoretical perspective, use of the FrFF or other similar methods may therefore be preferable in the context of processing kinematic and kinetic signals as a precursor to determining knee joint loads as well.

The retention of higher frequency content in kinematic and kinetic signals is further exemplified by representative time-series joint moment, GRF and lower limb accelerations during a single SS (Figure 4). For the FrFF, GRF and acceleration signals were closer to the unprocessed peak values during weight acceptance, and this higher-frequency content was also evident in the joint moments. While this suggests FrFF derived moments would be more accurate estimates of "true" knee moments, it is pertinent to comment on the source of these accelerations. GRFs from a force platform are relatively noise free compared to motion data (Lees & Lake, 2008), so matching the FrFF solution to the unprocessed peak vertical GRFs should be considered an improvement over the conventional approaches (Figure 4). It is plausible, however, some noisy oscillations were retained in FrFF marker accelerations that

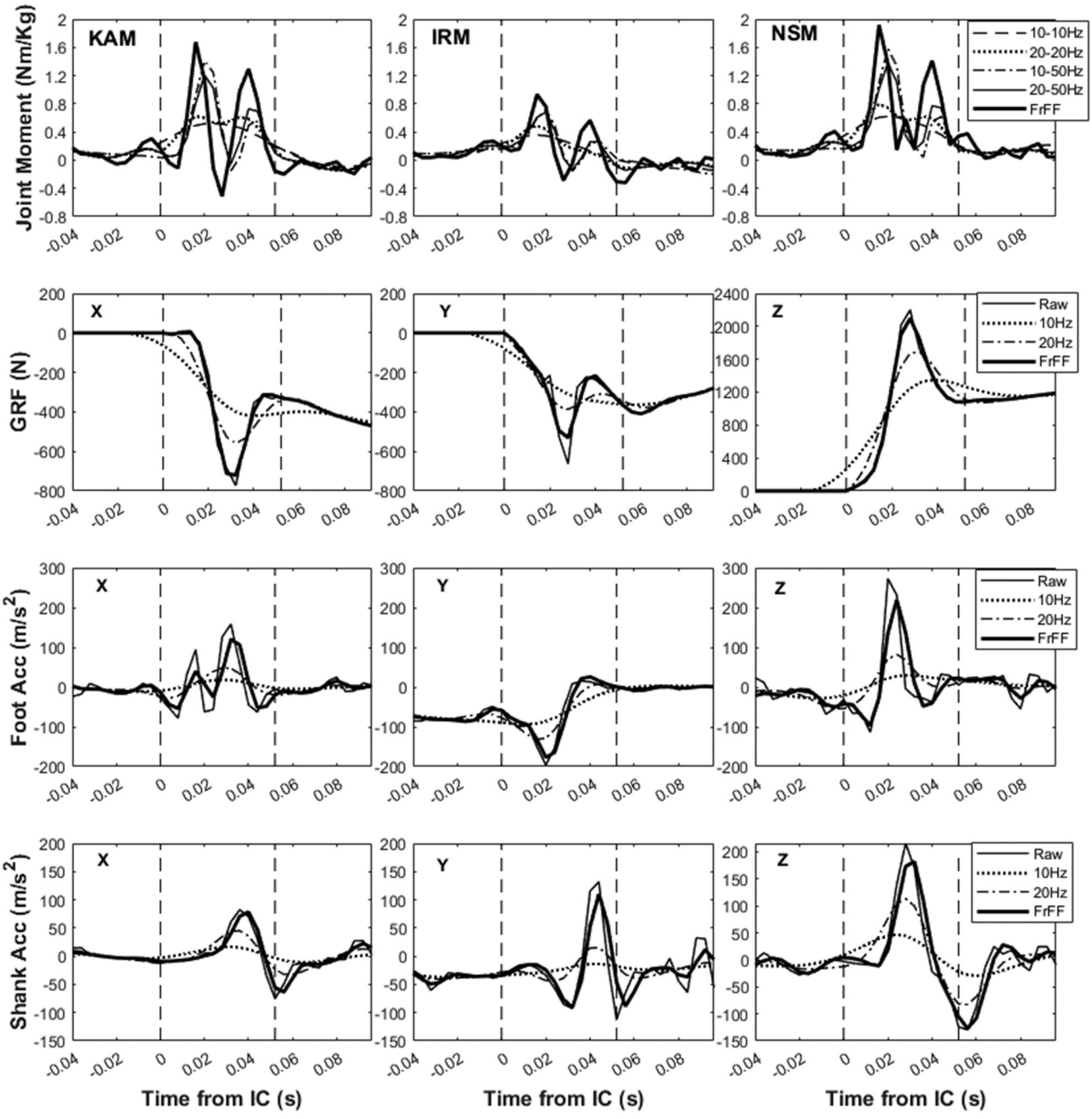

Figure 4. Representative knee abduction (KAM), internal rotation (IRM) and non-sagittal moments (NSM) (top row), ground reaction forces (second row), foot (third row) and shank (fourth row) centre of mass accelerations during an unanticipated side step. Vertical dashed lines at 0 s and 0.052 s indicate initial ground contact (IC) and the end of weight acceptance, respectively. X = medio-lateral, Y = anterior-posterior and Z = vertical.

propagated in the joint moments. It is thus difficult to imply FrFF derived knee moments were entirely representative of real joint loads. Evaluation of the FrFF with motion data with known intersegmental loads (e.g., van den Bogert & de Koning, 1996) is needed to verify this, and it is for these reasons Bisseling and Hof (2006) originally advocated using matched cut-off frequencies of ~20 hz to derive knee joint moments during dynamic sporting activity. Unfortunately, it is often overlooked they also advised low and matched cut-off frequencies should not be used if impact peak moments are of interest in relation to knee injuries. While matched approaches are suited to situations where general patterns of neuromuscular function are of interest (e.g., net moments during walking gait), situations that necessitate closer inspection of impact peak accelerations might benefit from using the FrFF.

Ideally, motion and GRF signals should be filtered at the highest frequency that removes noise yet leaves the physiologic signal intact (Derrick et al., 2020). The impact peak cut-off frequency for the FrFF was thus chosen to capture the entire range of lower-limb accelerations induced by foot-to-ground contact. It is important to note, however, that given variance in impact characteristics, optimal FrFF parameter selection may be task (and trial) specific. Compared to drop jumps, SS tasks are often performed at higher speeds, with larger foot-to-ground impact accelerations and subsequent knee joint loading (Kristianslund & Krosshaug, 2013;

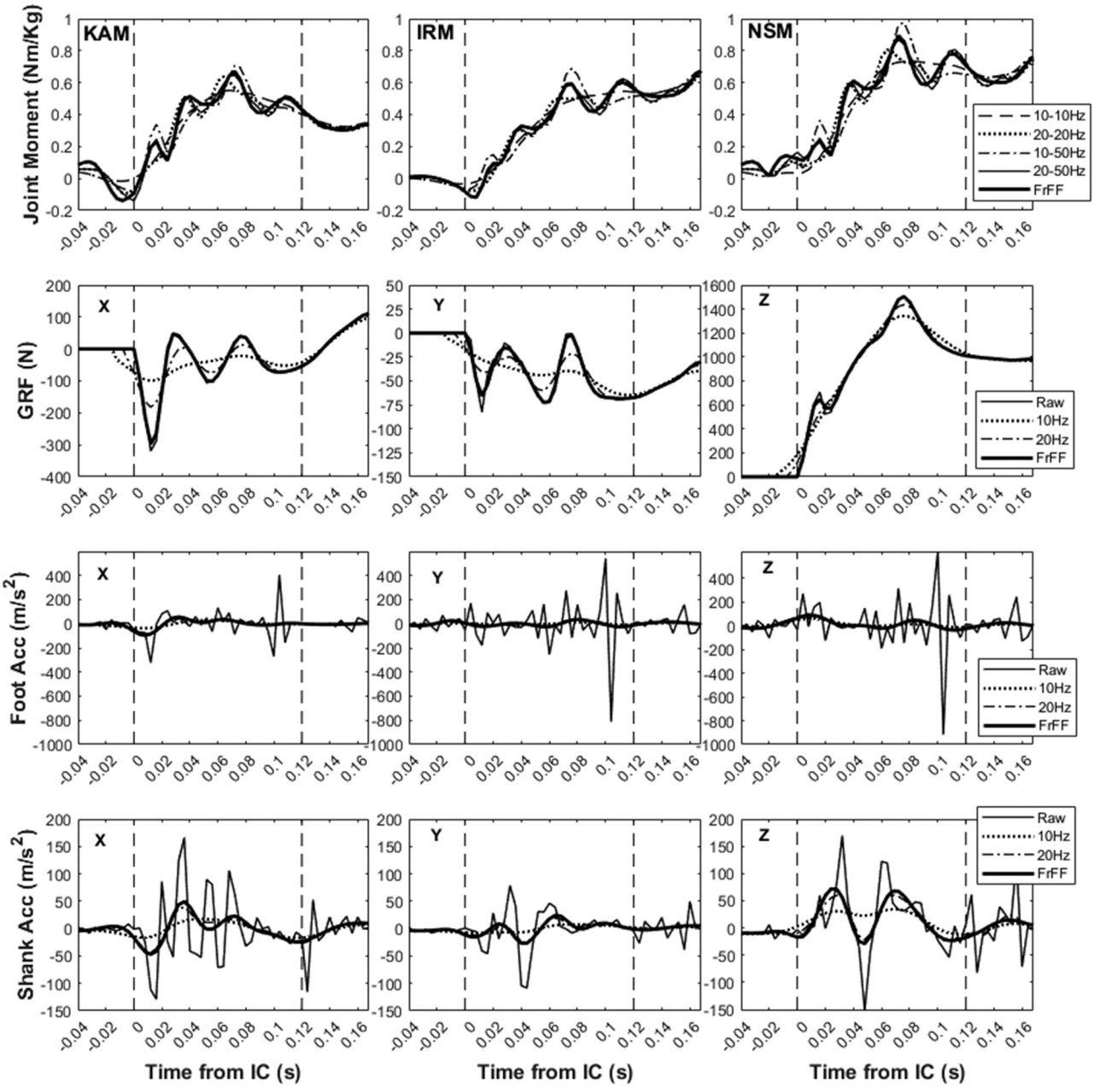

Figure 5. Representative knee abduction (KAM), internal rotation (IRM) and non-sagittal moments (NSM) (top row), ground reaction forces (second row), foot (third row row) and shank (fourth row) centre of mass accelerations during a bilateral drop jump. Vertical dashed lines at 0 s and 0.12 s indicate initial ground contact (IC) and the end of weight acceptance, respectively. X = medio-lateral, Y = anterior-posterior and Z = vertical.

Vanrenterghem et al., 2012). The largest differences in peak moments between the FrFF and conventional approaches was for the SS, indicating the FrFF was more sensitive to these impact peaks for these tasks. In contrast, differences between FrFF and conventional approaches were smaller for BDJ and SLDJ, and the 20–50 hz approach produced BDJ PKAM moments greater than the FrFF. Given high-frequency impact peaks are evident in drop jumping tasks (Kristianslund & Krosshaug, 2013), this was surprising. Interrogation of individual trials showed a longer weight acceptance phase in drop jumps (~0.12 s compared to ~0.05 s in SS) meant the FrFF did not always represent foot and shank kinematics in a manner that optimally retained high frequency kinematic content (Figure 5). The FrFF better represented GRFs than conventional approaches, but did not retain high frequency accelerations during weight acceptance. The peak moment estimates were thus closer in magnitude to conventional "unmatched" approaches.

Despite the highlighted variation in peak moments across filter approach and task, there was mostly moderate to excellent correlations between participant rankings (Table 3, Figure 3). Strong rank correlations have been previously shown between matched and unmatched filter approaches for PKAM during a similar SS task (Kristianslund et al., 2012), and the present study suggests consistency of the FrFF with these conventional approaches. The FrFF did show generally stronger rank correlations with unmatched compared to matched approaches during SS tasks, whereas correlations

were less variable for drop jump tasks. Importantly, this meant participants with the highest peak moment responses were identified as "at risk" irrespective of filter approach, and individual injury risk classifications were not drastically altered (Figure 2).

There were, however, some variation in risk classifications. For SS, matched approaches consistently excluded individuals that were identified as "at risk" in unmatched and FrFF approaches. This was most evident for 10–10 hz, suggesting all but the most aggressive filters were sensitive enough to identify athletes displaying elevated knee loads. Further, FrFF risk classifications were most consistent with 20–50 hz, indicating retention of high-frequency kinematic content is important for identifying "at risk" individuals (Roewer et al., 2014). Since a) all individual cases collectively identified by the conventional approaches were also identified by the FrFF and b) the FrFF identified some unique injury risk classifications (Figure 2), preliminary evidence is provided the FrFF displays enhanced sensitivity to movement strategies that induce higher knee loads during SS tasks. The proposed superiority of the FrFF over conventional approaches did not, however, extend to drop jumps. The previously highlighted inability of the FrFF to retain high frequency kinematic content during BDJ might explain this, and highlights a need to adjust FrFF parameters based on task specific foot-to-ground impact characteristics.

The frequency content that is accepted (and rejected) by the FrFF is ultimately determined by the gradient of the triangular cut-off boundary. Selecting an appropriate ratio between impact duration (width) and magnitude (peak cut-off value) becomes essential to obtain an optimal filter solution for a given rate of frequency expansion and reduction during the impact at hand. Since peak cut-off frequency values were unchanged across tasks, the longer weight acceptance durations for BDJ resulted in a shallower increase in cut-off frequencies on each side of the triangle and an inability to retain high-frequency acceleration and moment impact peaks (Figure 5). Peak cut-off frequency values other than 60 hz are thus likely optimal for bilateral drop jumping tasks. Further, given the absolute rate of expansion (and subsequent reduction) of marker frequency content around the peak impact frequency may not necessarily be equal, the isoscelean filter boundary of the FrFF might not be best suited in these instances (Georgakis & Subramaniam, 2009). Future work should thus attempt to optimise FrFF filter design and parameter selection across different ACL injury screening tasks to help improve estimates of knee loading. This might involve automatic filter parameter selection to minimise differences between unprocessed and FrFF signals (Georgakis & Subramaniam, 2009). While automating time-varying cut-off frequency filters in this way has proved difficult, it has been successfully achieved to improve filter performance in previous works (Davis & Challis, 2021; Georgakis et al., 2002).

Further limitations of the current study mean the findings should be regarded with some caution. Greater certainty regarding the origin of high-frequency accelerations in FrFF solutions, prospective injury registration data and comparison of the FrFF with known knee loading profiles are required to fully evaluate the FrFF's utility for classifying ACL injury risk. For the former, ideally the FrFF should be compared against other time-varying cut-off filtering methods as well (e.g., Davis & Challis, 2021). Given the aim of this study was to identify differences between the FrFF and conventionally used filter approaches, such a comparison was beyond the scope of this study. For the latter, a forward dynamic simulation of running has previously been used to identify exact lower-limb intersegmental loads with noise-free kinematics and compare data filtering approaches (van den Bogert & de Koning, 1996). Finally, FrFF performance should be evaluated in varied populations and across different screening tests. Interestingly, when the current sample was split by sex and analysed separately, similar patterns to those noted above emerged (see supplemental material).

In conclusion, the FrFF produced peak knee moment values during the weight acceptance phase of SS and drop jump tasks that were larger than those from "matched" approaches and closer to those from "unmatched" conventional filter approaches. Whilst the athletes with highest peak moment responses were classified as "at risk" irrespective of filter approach during sidestepping, matched approaches consistently excluded individual classifications compared to unmatched and FrFF approaches, and the FrFF identified unique classifications. Since the FrFF used a time-varying cut-off frequency to ensure a) important physiologic lower limb frequency content were retained in kinematic and GRF signals following foot-to-ground contact and b) consistency in the frequency content of these signals, preliminary evidence is provided the FrFF displays enhanced sensitivity to movement strategies that induce higher knee loads during SS tasks. This finding did not extend to drop jumps, and the FrFF should be further refined for use with these tasks. The FrFF's capability to identify "at risk" individuals who were excluded by conventional filter approaches is a key consideration for those performing ACL injury risk screening and/or prevention work using 3D motion capture. This is especially pertinent especially given the highlighted benefits of processing common ACL injury screening tasks using time-varying cut-off frequency filters. Ultimately, researchers and practitioners should carefully consider a) the influence different filter approaches (and their parameters) have on data interpretation and b) whether chosen filter approaches are appropriate for the context and/or variables under investigation.

Acknowledgments

The authors would like to thank Lucy Cooper for her assistance during data collection.

Disclosure statement

No potential conflict of interest was reported by the author(s).

Funding

The author(s) reported there is no funding associated with the work featured in this article.

ORCID

Simon Augustus http://orcid.org/0000-0001-9138-6962

References

Abram, S. G. F., Price, A. J., Judge, A., & Beard, D. J. (2018). Anterior cruciate ligament (ACL) reconstruction and meniscal repair rates have both increased in the past 20 years in England: Hospital statistics from 1997 to 2017. *British Journal of Sports Medicine*, *54*(5), 286–291. https://doi.org/10.1136/bjsports-2018-100195

Alonso, F. J., Castillo, J. M., & Pintado, P. (2005). Application of singular spectrum analysis to the smoothing of raw kinematic signals. *Journal of Biomechanics*, *38*(5), 1085–1092. https://doi.org/10.1016/j.jbiomech.2004.05.031

Augustus, S., Mithat Amca, A., Hudson, P. E., Smith, N. (2020). Improved accuracy of biomechanical motion data obtained during impacts using a time-frequency low-pass filter. *Journal of Biomechanics*, *101*, 109639. https://doi.org/10.1016/j.jbiomech.2020.109639

Augustus, S., & Smith, N. (2023). Changes in lower leg kinematic frequency content during pre-ground contact and weight acceptance phases of ACL injury risk screening tasks. *XXIX Congress of International Society of Biomechanics*, Fukuoka, Japan.

Bell, A. L., Pedersen, D. R., & Brand, R. A. (1990). A comparison of the accuracy of several hip center location prediction methods. *Journal of Biomechanics*, *23*(6), 617–621. https://doi.org/10.1016/0021-9290(90)90054-7

Bisseling, R. W., & Hof, A. L. (2006). Handling of impact forces in inverse dynamics. *Journal of Biomechanics*, *39*(13), 2438–2444. https://doi.org/10.1016/j.jbiomech.2005.07.021

Cappozzo, A., Catani, F., Della Croce, U., & Leardini, A. (1995). Position and orientation in space of bones during movement: Anatomical frame definition and determination. *Clinical Biomechanics*, *10*(4), 171–178. https://doi.org/10.1016/0268-0033(95)91394-T

Cerulli, G., Benoit, D. L., Lamontagne, M., Caraffa, A., & Liti, A. (2003). In vivo anterior cruciate ligament strain behaviour during a rapid deceleration movement: Case report. *Knee Surgery, Sports Traumatology, Arthroscopy*, *11*(5), 307–311. https://doi.org/10.1007/s00167-003-0403-6

Chinnasee, C., Weir, G., Sasimontonkul, S., Alderson, J., & Donnelly, C. (2018). A biomechanical comparison of single-leg landing and unplanned sidestepping. *International Journal of Sports Medicine*, *39*(8), 636–645. https://doi.org/10.1055/a-0592-7422

Cronström, A., Creaby, M. W., & Ageberg, E. (2020). Do knee abduction kinematics and kinetics predict future anterior cruciate ligament injury risk? A systematic review and meta-analysis of prospective studies. *BMC Musculoskeletal Disorders*, *21*(1), 1–11. https://doi.org/10.1186/s12891-020-03552-3

Davis, D. J., & Challis, J. H. (2021). Vertical ground reaction force estimation from benchmark nonstationary kinematic data. *Journal of Applied Biomechanics*, *37*(3), 272–276. https://doi.org/10.1123/jab.2020-0237

de Leva, P. (1996). Adjustments to Zatsiorky-Seluyanov's segment inertia parameters. *Journal of Biomechanics*, *29*(9), 1223–1230. https://doi.org/10.1016/0021-9290(95)00178-6

Derrick, T. R., van den Bogert, A. J., Cereatti, A., Dumas, R., Fantozzi, S., & Leardini, A. (2020). ISB recommendations on the reporting of intersegmental forces and moments during human motion analysis. *Journal of Biomechanics*, *99*, 109533. https://doi.org/10.1016/j.jbiomech.2019.109533

Filbay, S. R., Skou, S. T., Bullock, G. S., Le, C. Y., Räisänen, A. M., Toomey, C., Ezzat, A. M., Hayden, A., Culvenor, A. G., Whittaker, J. L., Roos, E. M., Crossley, K. M., Juhl, C. B., & Emery, C. (2022). Long-term quality of life, work limitation, physical activity, economic cost and disease burden following ACL and meniscal injury: A systematic review and meta-analysis for the OPTIKNEE consensus. *British Journal of Sports Medicine*, *56*(24), 1465–1474. https://doi.org/10.1136/bjsports-2022-105626

Georgakis, A., Stergioulas, L. K., & Giakas, G. (2002). Automatic algorithm for filtering kinematic signals with impacts in the Wigner representation. *Medical & Biological Engineering & Computing*, *40*(6), 625–633. https://doi.org/10.1007/BF02345300

Georgakis, A., & Subramaniam, S. R. (2009). Estimation of the second derivative of kinematic impact signals using fractional Fourier domain filtering. *IEEE Transactions on Biomedical Engineering*, *56*(4), 996–1004. https://doi.org/10.1109/TBME.2008.2006507

Hewett, T. E., Myer, G. D., Ford, K. R., Heidt, R. S., Jr., Colosimo, A. J., McLean, S. G., van den Bogert, A. J., Paterno, M. V., & Succop, P. (2005). Biomechanical measures of neuromuscular control and valgus loading of the knee predict anterior cruciate ligament injury risk in female athletes: A prospective study. *American Journal of Sports Medicine*, *33*(4), 492–501. https://doi.org/10.1177/0363546504269591

Kristianslund, E., & Krosshaug, T. (2013). Comparison of drop jumps and sport-specific sidestep cutting: Implications for anterior cruciate ligament injury risk screening. *American Journal of Sports Medicine*, *41*(3), 684–688. https://doi.org/10.1177/0363546512472043

Kristianslund, E., Krosshaug, T., & Van den Bogert, A. J. (2012). Effect of low pass filtering on joint moments from inverse dynamics: Implications for injury prevention. *Journal of Biomechanics*, *45*(4), 666–671. https://doi.org/10.1016/j.jbiomech.2011.12.011

Krosshaug, T., Nakamae, A., Boden, B. P., Engebretsen, L., Smith, G., Slauterbeck, J. R., Hewett, T. E., & Bahr, R. (2007). Mechanisms of anterior cruciate ligament injury in basketball: Video analysis of 39 cases. *American Journal of Sports Medicine*, *35*(3), 359–367. https://doi.org/10.1177/0363546506293899

Krosshaug, T., Steffen, K., Kristianslund, E., Nilstad, A., Mok, K. M., Myklebust, G., Andersen, T. E., Holme, I., Engebretsen, L., & Bahr, R. (2016). The vertical drop jump is a poor screening test for ACL injuries in female elite soccer and handball players: A prospective cohort study of 710 athletes. *American Journal of Sports Medicine*, *44*(4), 874–883. https://doi.org/10.1177/0363546515625048

Lees, A., & Lake, M. (2008). Force and pressure measurement. In C. Payton (Ed.), *Biomechanical evaluation of movement in sport and exercise : The British Association of Sport and Exercise Sciences guidelines* (pp. 53–77). Routledge.

Leppänen, M., Pasanen, K., Kujala, U. M., Vasankari, T., Kannus, P., Äyrämö, S., Krosshaug, T., Bahr, R., Avela, J., Perttunen, J., & Parkkari, J. (2017). Stiff landings are associated with increased ACL injury risk in young female basketball and floorball players. *American Journal of Sports Medicine*, *45*(2), 386–393. https://doi.org/10.1177/0363546516665810

Markolf, K. L., Burchfield, D. M., Shapiro, M. M., Shepard, M. F., Finerman, G. A., & Slauterbeck, J. L. (1995). Combined knee loading states that generate high anterior cruciate ligament forces. *Journal of Orthopaedic Research: Official Publication of the Orthopaedic Research Society*, *13*(6), 930–935. https://doi.org/10.1002/jor.1100130618

Myer, G. D., Ford, K. R., Paterno, M. V., Nick, T. G., & Hewett, T. E. (2008). The effects of generalized joint laxity on risk of anterior cruciate ligament injury in young female athletes. *American Journal of Sports Medicine*, *36*(6), 1073–1080. https://doi.org/10.1177/0363546507313572

Ozaktas, H. M., Kutay, M. A., & Mendlovic, D. (1999). Introduction to the fractional Fourier transform and its applications. In P. Hawkes (Ed.), *Advances in imaging and electron physics* (Vol. 106, pp. 239–291). Elsevier. https://doi.org/10.1016/S1076-5670(08)70272-6

Poulsen, E., Goncalves, G. H., Bricca, A., Roos, E., Thorlund, J. B., & Juhl, C. B. (2019). Knee osteoarthritis risk is increased 4-6 fold after knee injury—A systematic review and meta-analysis. *British Journal of Sports Medicine*, *53*(23), 1454–1463. https://doi.org/10.1136/bjsports-2018-100022

Robinson, M. A., Donnelly, C. J., Tsao, J., & Vanrenterghem, J. (2014). Impact of knee modeling approach on indicators and classification of anterior cruciate ligament injury risk. *Medicine & Science in Sports and Exercise*, *46*(7), 1269–1276. https://doi.org/10.1249/MSS.0000000000000236

Robinson, M. A., Sharir, R., Rafeeuddin, R., Vanrenterghem, J., & Donnelly, C. J. (2021). The non-sagittal knee moment vector identifies 'at risk' individuals that the knee abduction moment alone does not. *Sports Biomechanics*, *22*(1), 80–90. https://doi.org/10.1080/14763141.2021.1903981

Roewer, B. D., Ford, K. R., Myer, G. D., & Hewett, T. E. (2014). The 'impact' of force filtering cut-off frequency on the peak knee abduction moment during landing: Artefact or 'artifiction'? *British Journal of Sports Medicine*, *48*(6), 464–468. https://doi.org/10.1136/bjsports-2012-091398

Saxby, D. J., Catelli, D. S., Lloyd, D. G., & Sawacha, Z. (2023). Editorial: The role of biomechanics in anterior cruciate ligament injuries prevention. *Frontiers in Sports and Active Living*, *5*(1134969). https://doi.org/10.3389/fspor.2023.1134969

Sigward, S. M., & Powers, C. M. (2007). Loading characteristics of females exhibiting excessive valgus moments during cutting. *Clinical*

Biomechanics, *22*(7), 827–833. https://doi.org/10.1016/j.clinbiomech.2007.04.003

Toothaker, E. L. (1993). *Multiple comparison procedures*. SAGE Publications, Inc. https://doi.org/10.4135/9781412985178

Ueno, R., Navacchia, A., Bates, N. A., Schilaty, N. D., Krych, A. J., & Hewett, T. E. (2020). Analysis of internal knee forces allows for the prediction of rupture events in a clinically relevant model of anterior cruciate ligament injuries. *Orthopaedic Journal of Sports Medicine*, *8*(1), 1–13. https://doi.org/10.1177/2325967119893758

van den Bogert, A. J., & de Koning, J. J. (1996). On optimal filtering for inverse dynamics analysis. *Proceedings of the IXth Biennial Conference of the Canadian Society for Biomechanics* (pp. 214–215). Vancouver.

Vanrenterghem, J., Venables, E., Pataky, T., & Robinson, M. A. (2012). The effect of running speed on knee mechanical loading in females during side cutting. *Journal of Biomechanics*, *45*(14), 2444–2449. https://doi.org/10.1016/j.jbiomech.2012.06.029

Wachowiak, M. P., Rash, G. S., Quesada, P. M., & Desoky, A. H. (2000). Wavelet-based noise removal for biomechanical signals: A comparative study. *IEEE Transactions on Biomedical Engineering*, *47*(3), 360–368. https://doi.org/10.1109/10.827298

Wei, D., & Ran, Q. (2013). Multiplicative filtering in the fractional Fourier domain. *Signal, Image and Video Processing*, *7*(3), 575–580. https://doi.org/10.1007/s11760-011-0261-5

Weir, G. (2021). Anterior cruciate ligament injury prevention in sport: Biomechanically informed approaches. *Sports Biomechanics*, *00*(00), 1–21. https://doi.org/10.1080/14763141.2021.2016925

Weir, G., Alderson, J., Elliott, B., Lee, S., Devaprakash, D., Starre, K., Goodman, C., Cooke, J., Rechichi, C., Armstrong, J., Jackson, B., & Donnelly, C. (2019). A 2-yr biomechanically informed ACL injury prevention training intervention in female field hockey players. *Translational Journal of the American College of Sports Medicine*, *4*(19), 206. https://doi.org/10.1249/TJX.0000000000000105

Winter, D. A. (2009). *Biomechanics and motor control of human movement*. John Wiley & Sons.